Physica Medica 89 (2021) 226–231

Contents lists available at ScienceDirect

Physica Medica

journal homepage: www.elsevier.com/locate/ejmp

Original paper

Experimental investigation at CATANA facility of n-^{10}B and p-^{11}B reactions for the enhancement of proton therapy

D. Mazzucconi [a,b], D. Bortot [a,c,*], A. Pola [a,c], A. Fazzi [a,c], L. Cazzola [a], V. Conte [b], G.A.P. Cirrone [d], G. Petringa [d], G. Cuttone [d], L. Manti [e], S. Agosteo [a,c]

[a] Politecnico di Milano, Dipartimento di Energia, via La Masa 34, Milano, Italy
[b] INFN-Laboratori Nazionali di Legnaro, viale dell'Università 2, Legnaro, Padova, Italy
[c] INFN-sezione di Milano, via Celoria 16, Milano, Italy
[d] INFN-Laboratori Nazionali del Sud, via S. Sofia 62, Catania, Italy
[e] Dipartimento di Fisica "E. Pancini" Università degli Studi di Napoli Federico II & INFN-sezione di Napoli, Complesso Universitario di Monte S. Angelo, 80126 Napoli, Italy

ARTICLE INFO

Keywords:
Silicon telescope
Proton boron fusion reaction
Proton therapy
Boron neutron capture reaction

ABSTRACT

The aim of the NEPTUNE (Nuclear process-driven Enhancement of Proton Therapy UNravEled) project is to investigate in detail both the physical and radiobiological phenomena that could justify an increase of the proton-induced cytogenetic effects in cells irradiated in presence of an agent containing natural boron.

In this work, a double-stage silicon telescope coupled to different boron converters was irradiated at the CATANA proton therapy facility (INFN-LNS) for studying the proton boron fusion and the neutron boron capture reactions by discriminating secondary particles from primary protons.

Different boron targets were developed by depositing boric acid, enriched with a higher than 99% content of ^{10}B or ^{11}B, on a 50 μm thick PolyMethilMetacrylate (PMMA) substrate. The ^{10}B target allows to evaluate the contribution of lithium and alpha particles produced by the boron neutron capture reaction triggered by secondary thermal neutrons, while the ^{11}B target is exploited for studying the effect of the $p + {}^{11}B \rightarrow 3\alpha$ nuclear reaction directly triggered by primary protons.

Experimental results clearly show the presence of alpha particles from both the reactions. The silicon telescope is capable of discriminating, by means of the so-called "scatter plots", the contribution of alpha particles originated by thermal neutrons on ^{10}B with respect to the ones produced by protons impinging on ^{11}B. Although a reliable quantitative study of the alpha production rate has not been achieved yet, this work demonstrates that low energy and, therefore, high-LET particles from both the reactions can be measured.

1. Introduction

In the last decades, research on cancer radiotherapy included the so-called "hadrontherapy", a technique based on heavy charged particles, in particular protons and carbon ions [1]. The physical properties of such particles lead to a favorable depth-dose distribution and lower lateral spread with respect to photons and electrons. This, in principle, enables the delivery of very high-dose gradients close to organs at risk, confining the high-dose area to the tumor volume. The standard practice in proton therapy is to adopt a Relative Biological Effectiveness (RBE) constant value of 1.1 compared to photons in any clinical condition [2].

Safavi-Naeini et al. [3] proposed different methods for enhancing the radiation dose during hadron therapy by capturing thermal neutrons produced inside the treatment volume (Neutron Capture Enhanced Particle Therapy). One of the methods is based on the exploitation of common agents clinically used in Boron Neutron Capture Therapy (BNCT) for producing selectively high-LET helium and lithium ions inside the tumor cells via the thermal neutron capture reaction on ^{10}B.

On the other hand, Do-Kun et al. [4] proposed theoretically the idea to associate proton therapy with the nuclear fusion reaction produced by protons on ^{11}B, resulting in three alpha particles triggered by protons directly inside the tumoral cells: the local generation of high-LET particles could increase drastically the effectiveness of proton beams. Cirrone et al. [5] provided the first radiobiologically relevant proof of

* Corresponding author at: Politecnico di Milano, Dipartimento di Energia, via La Masa 34, Milano, Italy.
E-mail address: davide.bortot@polimi.it (D. Bortot).

https://doi.org/10.1016/j.ejmp.2021.08.008
Received 12 April 2021; Received in revised form 21 July 2021; Accepted 10 August 2021

Proton Boron Capture Therapy (PBCT): cells were irradiated with a clinical proton beam in the presence of sodium borocaptate ($Na_2B_{12}H_{11}SH$ or BSH) to selectively deliver given boron concentrations in cancer cells. In order to maximize the $p + {}^{11}B \rightarrow 3\alpha$ fusion rate, BSH with natural occurring boron isotopic abundance (i.e. about 80% in ^{11}B and 20% in ^{10}B) was used. In that work, a significant increase in proton-induced cytogenetic effects was observed, both in terms of cell death, assessed as loss of proliferative potential by the clonogenic assay, and of induction of complex DNA chromosome aberrations.

In light of these promising results, the National Italian Nuclear Physics Institute (INFN) funded the NEPTUNE (Nuclear process-driven Enhancement of Proton Therapy UNravEled) project for investigating in more details both the physical and radiobiological phenomena that could justify the measured increase of the proton-induced cytogenetic effects. In this framework, one of the working packages of the NEPTUNE project aimed at measuring microdosimetric spectra across the proton Bragg peak with tissue-equivalent proportional counters with boron-loaded or unloaded walls, and silicon microdosimeters covered on top by different boronated targets. The goal is the assessment of microdosimetric spectra at the same depths where biological samples are irradiated, in order to study the relation between biological effects and the physical characteristics of the radiation field, including the nuclear reactions.

In this work, a double-stage silicon telescope [6,7] coupled to different boron converters was irradiated at the CATANA proton irradiation line (INFN - Laboratori Nazionali del Sud, Catania, Italy), with the goal of studying the proton-boron and the neutron-boron reactions by discriminating produced particles from primary protons. Experimental results obtained with pure ^{10}B and ^{11}B are presented and discussed.

2. Materials and methods

2.1. The p-^{11}B and n-^{10}B nuclear reactions

The proton-boron nuclear reaction is formalized as $p + {}^{11}B \rightarrow 3\alpha$. It possesses a positive Q-value (8.7 MeV) and it is referred to as proton-boron fusion reaction. According to the literature [8], it shows three resonant energies and can be described as a two-step process in which three alpha particles are produced. A proton interacting with a ^{11}B nucleus induces the formation of a $^{12}C^*$ compound nucleus formed in the 2- or 3- excited state. $^{12}C^*$ then decays in one alpha particle and one ^{8}Be nucleus that, in turn, immediately decays in two secondary alpha particles, which exhibit a wide energy spectrum with a higher probability around 4 MeV. Such a reaction has been considered very attractive for the generation of fusion energy without producing neutron-induced radioactivity. As it was mentioned above, the p-^{11}B fusion reaction is expected to play a strategic role in medical applications improving the effectiveness of proton therapy, since 4 MeV alpha particles can stop completely in about 25 μm in tissue. More importantly, their LET far exceeds that of the primary proton beam, hence they are deemed to be more radiobiologically effective. The clinical relevance of this approach stems from the fact that the fusion reaction cross section becomes significantly high at relatively low incident proton energy (the main resonance is at 675 keV), i.e. across the Bragg peak region where tumor can be found in vivo.

The well-known BNCT reaction $n + {}^{10}B \rightarrow \alpha + {}^{7}Li$ is characterized by a very high cross section about 3800b (for thermal neutrons). Two high-LET particles are produced, i.e. a lithium ion and an alpha particle 0.84 MeV and 1.47 MeV in energy, respectively, together with a 0.48 MeV gamma ray (with a 94% probability). The lithium ion and the alpha particle energies are equal to 1.02 MeV and 1.78 MeV in the remaining 6%.

2.2. The double-stage silicon telescope

The silicon detector employed in this work is based on the monolithic telescope technology [9]. The standard structure consists of a ΔE stage and a residual-energy E stage about 1.9 μm and 500 μm in thickness, respectively. The sketch of the device is shown in Fig. 1. The ΔE stage acts as a solid state microdosimeter, while the E stage gives information on the energy of the impinging particle [6,10]. Both the E and ΔE stages are biased and the signals are collected separately in two different electronic chains. The amplified and shaped signals are acquired by a two-channel ADC in coincidence mode in order to keep the time correlation between the E and ΔE signals. The time resolution of the coincidence was 1 μs for minimizing the probability of pile up (lower than 10^{-4}). In this way, this telescope allows to discriminate the type of the impinging particle through the so-called "scatter-plot". Hence, the contribution of each particle to the microdosimetric distribution can be assessed.

If a microdosimetric spectrum comparable to that acquired with a reference Tissue-Equivalent Proportional Counter (TEPC) has to be determined, the distribution of the energy imparted in the ΔE elements should be corrected for tissue-equivalence. The use of a telescope detector, instead of a single stage, is justified by the role that the E stage plays for assessing the full energy of the impinging protons [6]. By recognizing each particle type and energy, the correction for the ratio of the stopping powers in tissue and in silicon is applied event by event. This tissue-equivalence conversion procedure has been successfully applied for measuring proton microdosimetric distributions, which resulted to be comparable to those produced by a cylindrical reference mini-TEPC at lineal energies higher than 8 keV/μm [11,12] which corresponds to the minimum signal that the silicon telescope can detect.

2.3. Boron targets

Different boron targets were designed and developed at the Politecnico di Milano by depositing boric acid (H_3BO_2), both enriched up to over 99% in ^{11}B or ^{10}B, on a 50 μm thick PolyMethilMetacrylate (PMMA) substrate. The compound was deposited through an evaporation process based on the preparation of an aqueous solution of the selected compound. The boric acid has been adopted for two reasons: i) the deposition process requires a water-soluble molecule; ii) both ^{11}B and ^{10}B enriched compounds are available in the same chemical form. As discussed below, the ^{10}B enriched target is fundamental for evaluating the contribution of alpha particles produced by the boron neutron capture reaction $^{10}B(n,\alpha)^{7}Li$. It should be mentioned that a 0.48 MeV gamma ray is produced with a probability of 94%.

A picture of the PMMA substrate with the deposition of the boron compound (white powder) is shown in Fig. 2.

2.4. CATANA proton irradiation beamline and experimental set-up

The CATANA therapeutic facility at the LNS - INFN is based on a 62 MeV proton beam and a passive half-modulated Spread Out Bragg Peak (SOBP) to treat ocular melanomas [13]. Measurements were performed at 30.3 mm in water depth across the SOBP, as reported in Fig. 3, left side. This depth has been obtained by introducing a PMMA (Polymethylmethacrylate) slab upstream of the converter. This position was selected in order to maximize the alpha particle production, according to the reaction cross section. Three measurements were performed: without any boron (i.e. with the 50 μm PMMA substrate only), with the ^{11}B enriched target and with the ^{10}B enriched target.

The boron enriched target was placed in front of the sensitive region of the silicon telescope (i.e. ΔE stage) as reported in Fig. 3, right side. The distance between the detector and the target was around 1 mm in air.

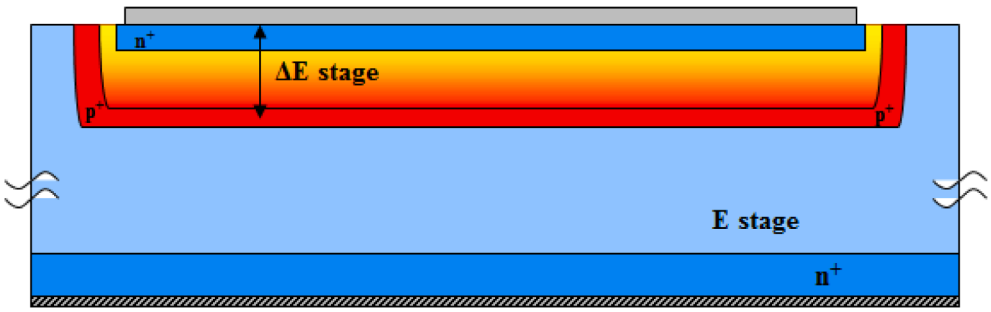

Fig. 1. Scheme of the monolithic silicon telescope.

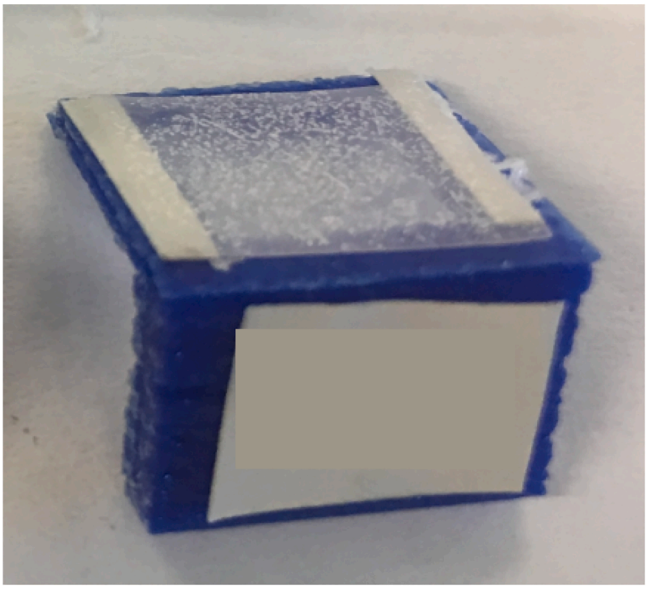

Fig. 2. Picture of the PMMA substrate where the boric acid, enriched in ^{11}B or ^{10}B, was deposited on. The blue plastic support is needed for the manipulation and the positioning of the target. (For interpretation of the references to colour in this figure legend, the reader is referred to the web version of this article.)

3. Results and discussion

The scatter-plots obtained without boron converter and with the ^{10}B and ^{11}B enriched targets are shown in Fig. 4. The abscissa axis represents the total energy deposited in the silicon telescope (sum of ΔE and E stages), while the ordinate axis shows the energy deposited in the ΔE stage only. These scatter-plots have been normalized to the total number of events. From the stopping-power tables relative to silicon for protons and alpha particles [14], theoretical curves can be drawn on the scatter-plots. Since the detector is positioned at the end of the SOBP, it is assumed that both alpha particles and protons come to a complete halt in the E stage (500 μm). These analytical curves help to identify the species of the particles on the scatter plot. In fact, the observed proton distribution follows the theoretical curve, represented by the black line. Moreover, low energy particles stop completely in the ΔE stage and, therefore, their points lay on the bisector of the scatter-plot, since the total energy is given by the ΔE stage only.

By examining the alpha particle analytical curve (red line in the figures), some differences are noticed. In the absence of any converter, there can be seen few points around the red line. They may be due to recoil ions from nuclear elastic or inelastic reaction of protons with the detector itself or the surrounding materials (e.g. the target substrate). It should be mentioned that the p^+ dopant separating the two stages of the silicon telescope was made by implanting ^{11}B and therefore these events may also be ascribed to alpha particles from the (p,3α) reaction. In contrast, the scatter-plot related to the ^{10}B converter presents a population of alpha particles characterized by a total energy around 1 MeV and a relatively high imparted energy to the ΔE stage, higher than 500 keV. These alpha particles are due to the ^{10}B neutron capture reaction induced by thermal neutrons that are generated by high-energy neutrons scattering mainly in the concrete shielding barriers of the treatment room. These secondary high-energy neutrons are produced by the primary proton beam interacting (via intra-nuclear cascade reactions) with the structural materials of the dose delivery system (collimators, range modulator, the PMMA phantom, etc.). Realistically,

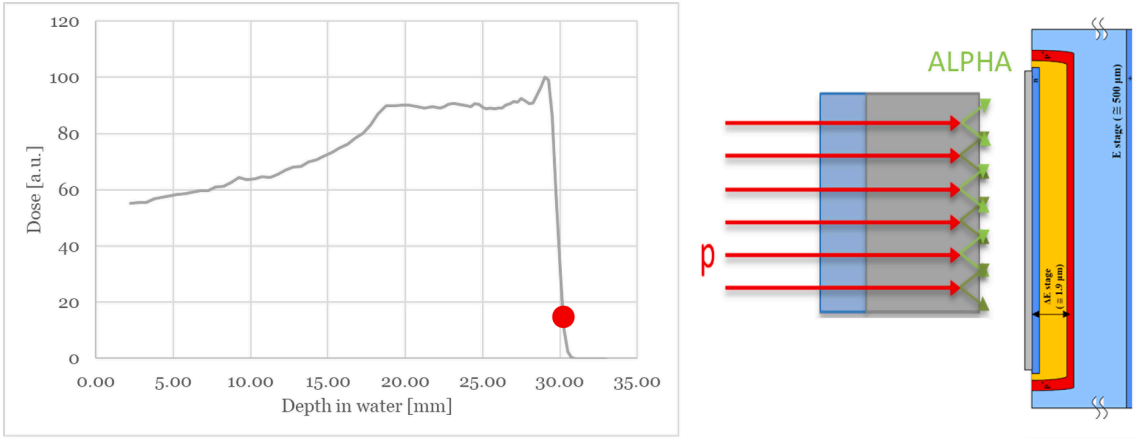

Fig. 3. Left side: depth-dose profile of the CATANA proton beamline. The red dot represents the point at which the silicon telescope was placed. Right side: scheme of the experimental set-up of the boron target (gray) deposited on its PMMA substrate (blue), together with the silicon telescope structure (not to scale). (For interpretation of the references to colour in this figure legend, the reader is referred to the web version of this article.)

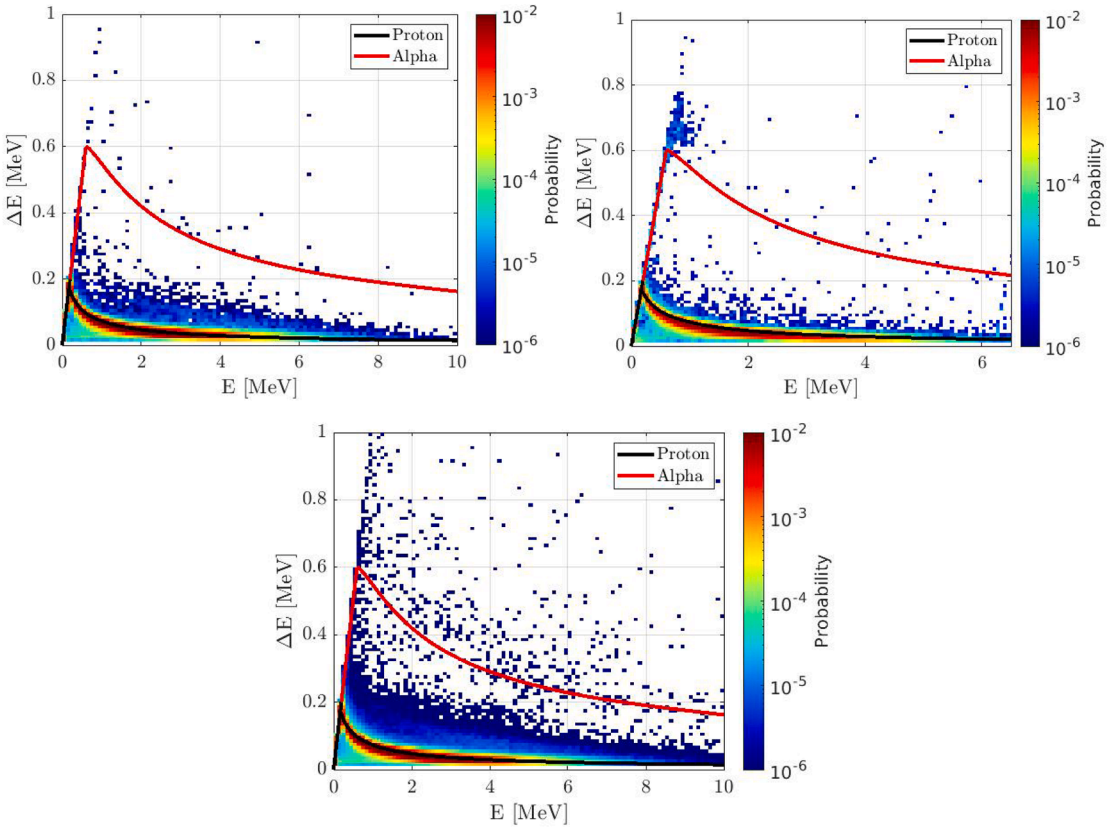

Fig. 4. Scatter-plots measured by the silicon telescope without any converter (up, left), with the ^{10}B converter (up, right) and with the ^{11}B converter (bottom), normalized to the total number of events. Black and red lines represent the analytical distributions of protons and alpha particles, respectively. (For interpretation of the references to colour in this figure legend, the reader is referred to the web version of this article.)

many lithium ions are self-absorbed in the target due to the lower energy and lower range and therefore most of the signals in the silicon detector are given by alpha particles. Nevertheless, the possible overlap between alpha and lithium signals would be concentrated in the bisector of the scatter plot. It should be observed that the population of alpha events is slightly above the theoretical curve. This may be due to the fact that the products of the ^{10}B capture reaction are emitted in opposite directions and with an isotropic angular distribution and therefore they can travel more than 1.9 μm inside the ΔE stage (depositing more energy than expected with theoretical calculations).

The scatter-plot measured with the ^{11}B converter presents a broad distribution of events around locus on a scatter plot corresponding to alpha particles. This distribution is likely related to the products of the p-^{11}B reaction in the converter. The distribution of alpha particles is broad around the analytical line for two possible reasons: i) the ΔE-E telescope cannot discriminate events due to more than one alpha particle produced in the same reaction; ii) the alpha particle track is generally longer than the ΔE thickness, because its emission direction may be not perpendicular to the detector surface.

By exploiting the scatter-plots, it is possible to discriminate events due to alpha particles produced in the boron target from primary protons traversing the target itself, for both the ^{10}B and ^{11}B converters. This can be achieved by defining a proper threshold curve in the scatter-plots: this is calculated by averaging the ΔE values of the analytical curves of protons and alpha particles for each E value. The result is a threshold which lies between the two analytical trends. This discrimination allows to evaluate the energy distribution of the alpha particles and their imparted energy in the ΔE stage. These results are plotted in Fig. 5. As previously described, the total energy spectrum of alpha particles from ^{10}B is peaked around 1 MeV. Consequently, the energy imparted in the ΔE stage (Fig. 5, top left) is rather high and its mean is equal to 580 keV.

On the other hand, the energy spectrum of the alpha particles emitted by the proton-boron fusion reaction is broader and shows an endpoint around 7 MeV. The spectrum of the imparted energy given in the ΔE stage is also broader and its mean value is equal to 520 keV.

At this state of the investigation, a first estimation of the ratios of alpha particles with respect to the protons is: $7.6{\cdot}10^{-5} \pm 23.6\%$ without any converter, $1.0{\cdot}10^{-3} \pm 9.8\%$ for ^{10}B and $1.2{\cdot}10^{-4} \pm 7.0\%$ for ^{11}B. The reported uncertainties are referred to a confidence interval of about 95%. It should be underlined that a more reliable evaluation about the production rate of alpha particles with respect to the impinging primary protons is hard to achieve, since the amount of boron atoms in the targets cannot be estimated with a reasonable uncertainty.

By applying the event-by-event tissue-equivalent correction [6] to the alpha particle spectra in the ΔE stage, based on the stopping power tables (for silicon and for liquid water) and considering, as a first approximation, the conventional definition of the mean chord length for a convex body [15], equal to 3.79 μm, the microdosimetric distribution of the alpha particles can be derived and it is depicted in Fig. 6.

The dose-mean lineal energies for ^{10}B and ^{11}B alpha particles are 120.4 keV/μm ± 23.0% and 122.2 keV/μm ± 13.0%, respectively. The reported uncertainties are referred to a confidence interval of about 95%. This result highlights the high efficiency in creating complex damages to cells also for the alpha particles coming from the proton-boron fusion reaction.

4. Conclusions

In this work, the investigation of the proton induced reaction on boron has been carried out through a double-stage silicon telescope alternatively coupled to three targets coated with different boron content: no boron, pure ^{10}B or pure ^{11}B. The multiple measurements allow

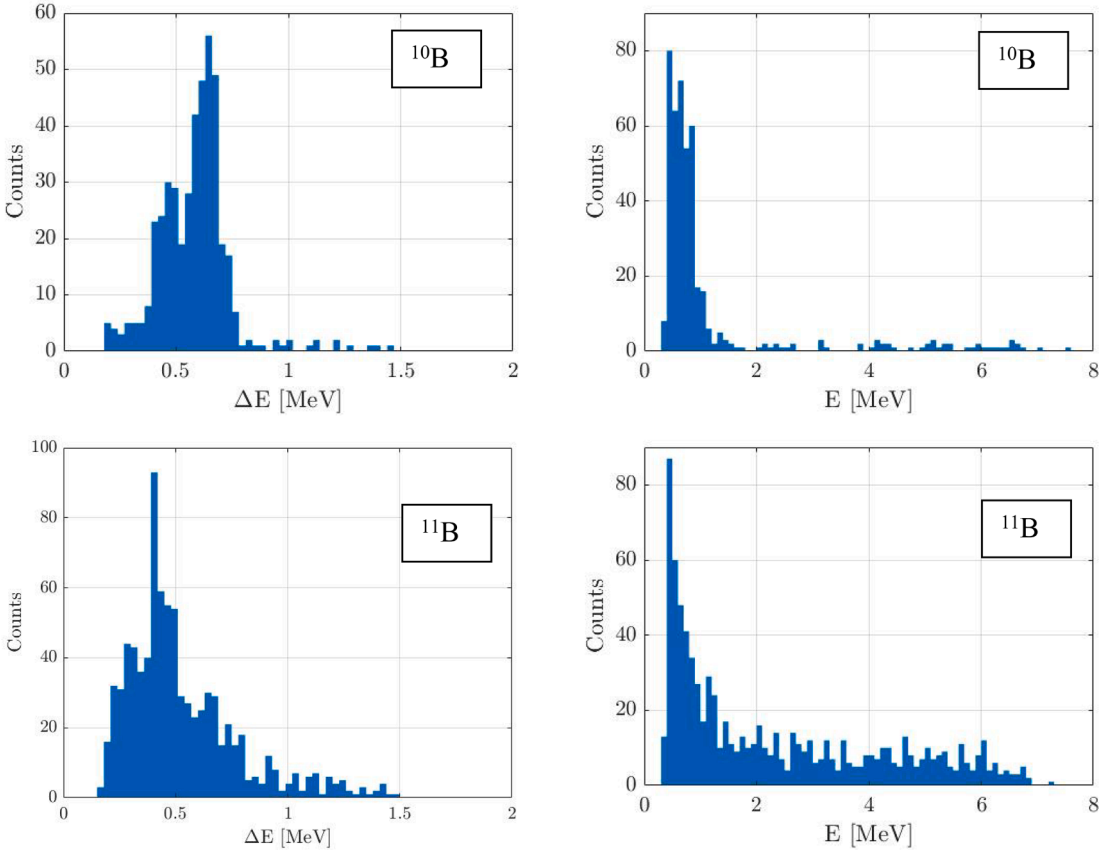

Fig. 5. Imparted energy in the ΔE stage and energy spectra of alpha particles measured with ^{10}B converter (top left and top right, respectively) and with ^{11}B converter (bottom left and bottom right, respectively).

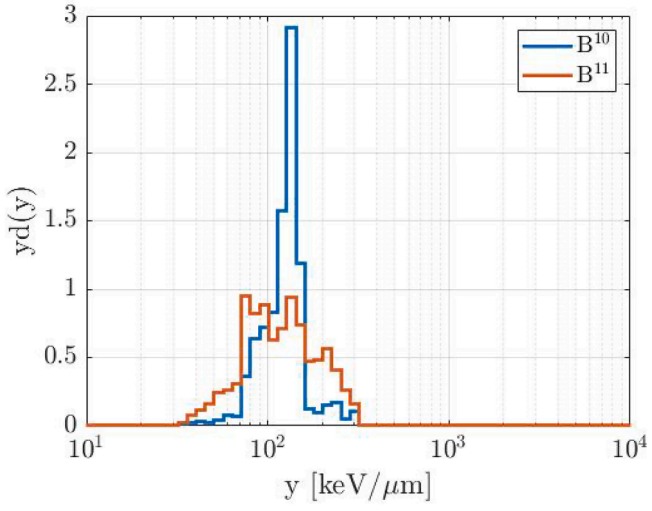

Fig. 6. Microdosimetric distributions of alpha particles obtained with the ^{10}B and ^{11}B converters.

to discriminate the contribution of alpha particles from thermal neutron capture on ^{10}B from the ones generated by protons impinging on ^{11}B atoms. The boronated targets were developed by means of an evaporation deposition technique on a PMMA substrate by using boric acid enriched in ^{10}B and ^{11}B, respectively.

The irradiations were performed at the CATANA proton beam line by exploiting a clinical SOBP for the treatment of eye melanoma. The silicon telescope coupled with the target was placed at the end of the depth-dose distribution, since the reaction cross sections of the p-^{11}B fusion reaction exhibits some resonances for low energy protons (the main resonance is at 675 keV). The detector was irradiated without any converter and with the two boron targets. The results show that alpha particles were detected for both the converters: alpha particles derive from both the boron neutron thermal capture (target enriched in ^{10}B) and from the p-^{11}B fusion reaction (target enriched in ^{11}B).

It should be stressed that, at this point of the research and for this preliminary irradiation campaign, a reliable quantitative evaluation about the production rate of alpha particles with respect to primary protons is hard to achieve, since the amount of boron atoms in the targets cannot be estimated with a reasonable uncertainty. In fact, the quantitative values given in this paper are simply evaluated on the experimental scatter plots. Moreover, this complex radiation field and the adopted irradiation set-up prevent the assessment of the alpha detection efficiency.

Nevertheless, this work demonstrates that low energy and, therefore, high-LET alpha particles from the fusion reaction triggered by low energy protons on the ^{11}B can be measured. Moreover, the thermal neutron field induced by the primary proton beam leads to a discrete amount of ^{10}B capture reactions. In the next future, dedicated experiments are foreseen for a quantitative analysis on the production rate. These experimental campaigns will adopt proper targets with a well-known boron atom density and a dedicated set-up in which the detection efficiency of the silicon telescope can be assessed. Moreover, Monte Carlo simulations are foreseen for a direct comparison with the experimental results.

Acknowledgements

This work was supported by the Italian National Institute for Nuclear

Physics - INFN - Scientific Commission V in the framework of the NEPTUNE (Nuclear process-driven Enhancement of Proton Therapy UNravEled) experiment.

References

[1] Loeffler JS, Durante M. Charged particle therapy–optimization, challenges and future directions. Nat Rev Clin Oncol 2013;10(7):411–24. https://doi.org/10.1038/nrclinonc.2013.79.

[2] ICRU. Prescribing, Recording, and Reporting Proton-Beam Therapy. ICRU 2007; report 78.

[3] Safavi-Naeini M, Chacon A, Guatelli S, Franklin DR, Bambery K, Gregoire M-C, et al. Opportunistic dose amplification for proton and carbon ion therapy via capture of internally generated thermal neutrons. Sci Rep 2018;8(1). https://doi.org/10.1038/s41598-018-34643-w.

[4] Yoon D-K, Jung J-Y, Suh TS. Application of proton boron fusion reaction to radiation therapy: A Monte Carlo simulation study. Appl Phys Lett 2014;105(22):223507. https://doi.org/10.1063/1.4903345.

[5] Cirrone GAP, Manti L, Margarone D, Petringa G, Giuffrida L, Minopoli A, et al. First experimental proof of Proton Boron Capture Therapy (PBCT) to enhance protontherapy effectiveness. Sci Rep 2018;8(1). https://doi.org/10.1038/s41598-018-19258-5.

[6] Agosteo S, Cirrone GAP, Colautti P, Cuttone G, D'Angelo G, Fazzi A, et al. Study of a silicon telescope for solid state microdosimetry: preliminary measurements at the therapeutic proton beam line of CATANA. Radiat Meas 2010;45(10):1284–9. https://doi.org/10.1016/j.radmeas.2010.06.051.

[7] Pola A, Bortot D, Mazzucconi D, Fazzi A, Galer S, Kirkby KJ, et al. Characterization of a pixelated silicon microdosimeter in microbeams of light ions. Radiat Meas 2020;133:106296. https://doi.org/10.1016/j.radmeas.2020.106296.

[8] Spraker MC, Ahmed MW, Blackston MA, Brown N, France III RH, Henshaw SS, et al. The 11B(p, α)8Be → α + α and the 11B(α, α)11B reactions at energies below 5.4 MeV. J Fusion Energ 2012;31:357–67. https://doi.org/10.1007/s10894-011-9473-5.

[9] Tudisco S, Amorini F, Cabibbo M, Cardella G, De Geronimo G, Di Pietro A, et al. A new large area monolithic silicon telescope. Nucl Instrum Meth A 1999;426(2-3):436–45.

[10] Agosteo S, Fallica PG, Fazzi A, Introini MV, Pola A, Valvo G. A pixelated silicon telescope for solid state microdosimetry. Radiat Meas 2008;43(2-6):585–9. https://doi.org/10.1016/j.radmeas.2007.12.053.

[11] Bianchi A, Selva A, Colautti P, Bortot D, Mazzucconi D, Pola A, et al. Microdosimetry with a sealed mini-TEPC and a silicon telescope at a clinical proton SOBP of CATANA. Radiat Phys Chem 2020;171:108730. https://doi.org/10.1016/j.radphyschem.2020.108730.

[12] Colautti P, Bianchi A, Selva A, Bortot D, Mazzucconi D, Pola A, et al. Therapeutic proton beams: LET, RBE and microdosimetric spectra with gas and silicon detectors. Radiat Meas 2020;136:106386. https://doi.org/10.1016/j.radmeas.2020.106386.

[13] Cirrone GAP, Cuttone G, Lojacono PA, Lo Nigro S, Mongelli V, Patti IV, et al. A 62 MeV proton beam for the treatment of ocular melanoma at Laboratori Nazionali del Sud-INFN. IEEE Trans Nucl Sci 2004;51:860–5. https://doi.org/10.1109/TNS.2004.829535.

[14] Ziegler JF, Ziegler MD, Biersack JP. SRIM the stopping and range of ions in matter. Nucl Instrum Methods B 2010;268:1818–23. https://doi.org/10.1016/j.nimb.2010.02.091.

[15] ICRU. Microdosimetry. ICRU 1983; report 36.